

ACCEPTED MANUSCRIPT • OPEN ACCESS

# High-current, high-voltage AlN Schottky Barrier Diodes

To cite this article before publication: Cris E Quiñones *et al* 2024 *Appl. Phys. Express* in press <https://doi.org/10.35848/1882-0786/ad81c9>

## Manuscript version: Accepted Manuscript

Accepted Manuscript is “the version of the article accepted for publication including all changes made as a result of the peer review process, and which may also include the addition to the article by IOP Publishing of a header, an article ID, a cover sheet and/or an ‘Accepted Manuscript’ watermark, but excluding any other editing, typesetting or other changes made by IOP Publishing and/or its licensors”

This Accepted Manuscript is © 2024 The Author(s). Published on behalf of The Japan Society of Applied Physics by IOP Publishing Ltd.



As the Version of Record of this article is going to be / has been published on a gold open access basis under a CC BY 4.0 licence, this Accepted Manuscript is available for reuse under a CC BY 4.0 licence immediately.

Everyone is permitted to use all or part of the original content in this article, provided that they adhere to all the terms of the licence <https://creativecommons.org/licenses/by/4.0>

Although reasonable endeavours have been taken to obtain all necessary permissions from third parties to include their copyrighted content within this article, their full citation and copyright line may not be present in this Accepted Manuscript version. Before using any content from this article, please refer to the Version of Record on IOPscience once published for full citation and copyright details, as permissions may be required. All third party content is fully copyright protected and is not published on a gold open access basis under a CC BY licence, unless that is specifically stated in the figure caption in the Version of Record.

View the [article online](#) for updates and enhancements.

# High-current, high-voltage AlN Schottky Barrier Diodes

C. E. Quiñones,<sup>1\*</sup> D. Khachariya,<sup>2</sup> P. Reddy,<sup>2</sup> S. Mita,<sup>2</sup> J. Almeter,<sup>1</sup>  
P. Bagheri,<sup>1</sup> S. Rathkanthiwar,<sup>1</sup> R. Kirste,<sup>2</sup> S. Pavlidis,<sup>3</sup> E. Kohn,<sup>2</sup> R.  
Collazo,<sup>1</sup> and Z. Sitar<sup>1,2</sup>

<sup>1</sup> Department of Materials Science and Engineering at North Carolina State University, Raleigh, NC 27606

USA<sup>2</sup>Adroit Materials, Cary, NC 27518, USA

<sup>3</sup>Department of Electrical and Computer Engineering, North Carolina State University, Raleigh, NC 27606, USA.

\*Corresponding author's email address: cequinon@ncsu.edu

AlN Schottky barrier diodes with low ideality factor ( $<1.2$ ), low differential ON-resistance ( $<0.6 \text{ m}\Omega\cdot\text{cm}^2$ ), high current density ( $>5 \text{ kA/cm}^2$ ), and high breakdown voltage (680 V) are reported. The device structure consisted of a two-layer, quasi-vertical design with a lightly doped AlN drift layer and a highly doped  $\text{Al}_{0.75}\text{Ga}_{0.25}\text{N}$  ohmic contact layer grown on AlN substrates. A combination of simulation, current-voltage measurements, and impedance spectroscopy analysis revealed that the AlN/AlGa<sub>N</sub> interface introduces a parasitic electron barrier due to the conduction band offset between the two materials. This barrier was found to limit the forward current in fabricated diodes. Further, we show that introducing a compositionally-graded layer between the AlN and the AlGa<sub>N</sub> reduces the interfacial barrier and increases the forward current density of fabricated diodes by a factor of  $10^4$ .

Aluminum nitride (AlN) has the potential for realizing semiconductor power devices with breakdown voltages  $>10 \text{ kV}$ , ideal for applications in high-voltage, direct-current (HVDC) power transmission and locomotive drive systems.<sup>1</sup> Due to its high breakdown field ( $>16 \text{ MV/cm}$ ) and high electron mobility,<sup>2-4</sup> AlN has a Baliga figure of merit (BFOM)  $>30\times$  larger than that of GaN or SiC. Devices based on AlN with breakdown voltages in the  $10 \text{ kV}$  range would require drift layers only a few micrometers thick. Operating at higher frequencies than standard Si-based power switching technology, such devices would eliminate the need for bulky transformers in power transmission systems and greatly reduce their size and cost. However, such applications require AlN-based devices capable of passing  $\text{kA/cm}^2$  of current in forward bias (with little to no loss), while simultaneously blocking electric fields on the order of  $\text{MV/cm}$  in reverse bias. The state-of-the-art performance is currently far from the requirements for these applications.

The main obstacle for achieving better performance in AlN devices has been the lack of controllable doping. N-type doping is difficult in AlN because donors tend to have very high activation energies ( $>250 \text{ meV}$ ) and are easily compensated due to low formation energies of compensating point defects.<sup>5-7</sup> Because of this, alternative doping schemes have been explored, such as distributed polarization doping in compositionally-graded AlGa<sub>N</sub> films.<sup>8-12</sup> Recently, this method has been used to demonstrate high forward current density in AlGa<sub>N</sub> p-n diodes on AlN substrates.<sup>13</sup> In parallel, conventional doping techniques were advanced by the development of point defect management frameworks in the III-nitrides, that have allowed for a systematic suppression of self-compensation in

these materials.<sup>14,15</sup> Using these methods, controllable n-type conductivity in Si-doped AlN with electron mobilities exceeding  $300 \text{ cm}^2/\text{Vs}$  have been demonstrated.<sup>16–20</sup>

Building on these developments, we have recently demonstrated near-ideal behavior of lateral AlN Schottky diodes that were stable up to  $700^\circ\text{C}$ .<sup>21</sup> Additionally, other groups have reported on high-voltage AlN Schottky barrier diodes with blocking voltages  $>3 \text{ kV}$ .<sup>22,23</sup> Although these are promising results that show the potential of the AlN technology, the forward current densities in these devices were far from practical. To the best of our knowledge, the highest reported current density in an AlN SBD is by Maeda et al.<sup>24</sup> with  $\sim 1 \text{ A/cm}^2$ . However, most reports on AlN Schottky diodes found in the literature show room temperature current densities on the order of  $10^{-3}$  to  $10^{-1} \text{ A/cm}^2$ .<sup>21–27</sup> In this letter, we implement a compositionally-graded layer to the AlN drift region that enabled more than 3 orders of magnitude higher current density than the current state-of-the-art for AlN Schottky barrier diodes. The diodes sustain forward current densities  $>1 \text{ kA/cm}^2$ , while simultaneously blocking reverse voltage of  $680 \text{ V}$ .

To achieve desired device performance, formation of low resistance ohmic contacts is crucial. For this purpose, we implemented a quasi-vertical structure comprising a heavily-doped AlGa<sub>x</sub>N layer as a contact layer. Low resistance ohmic contacts to conductive high Al-content Al<sub>x</sub>Ga<sub>1-x</sub>N with specific contact resistance on the order of  $10^{-6} \Omega \cdot \text{cm}^2$  can be reliably achieved.<sup>28,29</sup> Further, conductive high Al-content AlGa<sub>x</sub>N epilayers of thickness  $>3 \mu\text{m}$  can be pseudomorphically grown on native AlN substrates, making this an attractive choice for a current spreading layer in a quasi-vertical AlN Schottky barrier diode.<sup>30</sup> However, the AlN/Al<sub>x</sub>Ga<sub>1-x</sub>N heterojunction introduces an electron barrier at this interface and severely limits the forward current in fabricated devices.

To illustrate the effect of the AlN/AlGa<sub>x</sub>N interface on device performance, two device structures were simulated using Silvaco TCAD: a device with an abrupt heterojunction and a device with a graded-layer heterojunction. Their schematic cross sections are shown in Figs. 1(a) and 1(b). Both devices consisted of an n<sup>+</sup>-AlN drift layer and an n<sup>+</sup>-Al<sub>0.75</sub>Ga<sub>0.25</sub>N contact layer with [Si] of  $1 \times 10^{18}$  and  $1 \times 10^{19} \text{ cm}^{-3}$ , respectively. The simulated equilibrium band structures around the heterojunction are shown for both cases in Fig. 1(c). The Si ionization energy is taken to be  $0.3 \text{ eV}$  and  $0.07 \text{ eV}$  in AlN and Al<sub>0.75</sub>Ga<sub>0.25</sub>N, respectively. This results in a room temperature carrier concentration on the order of  $10^{15}$  and  $10^{18} \text{ cm}^{-3}$  in the AlN and the AlGa<sub>x</sub>N, respectively. For the abrupt heterojunction, there is a sharp discontinuity at the interface due to the conduction band offset between the materials. This introduces an electron barrier for electrons flowing from the AlGa<sub>x</sub>N into the AlN. This electron barrier is reverse biased when the Schottky barrier is forward biased and acts as a non-linear series impedance when the Schottky barrier turns on. In contrast, for the graded-layer heterojunction device, the conduction band is pulled down close to the Fermi level because of the bound polarization charge, and there is no electron barrier. The simulated  $I$ - $V$ s of the two devices are shown in Fig. 1(c). The graded-layer heterojunction diode shows superior ON-state performance, with around three orders of magnitude higher current density compared to the abrupt heterojunction diode. The results of this simulation suggest that high forward current density can be achieved by using a compositionally-graded interlayer to manage the band offset at the AlN/AlGa<sub>x</sub>N interface.

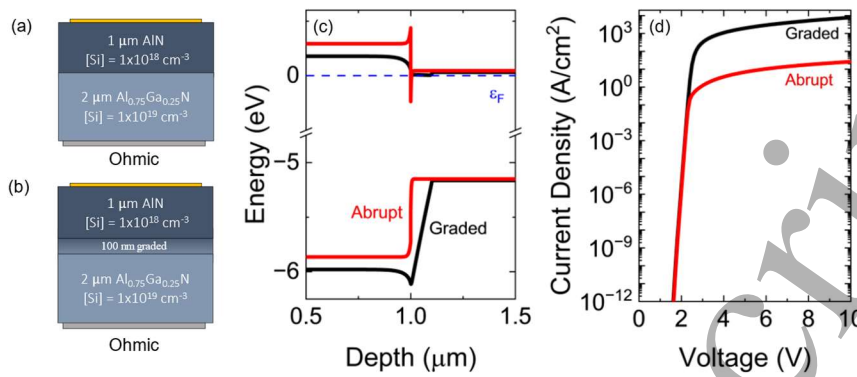


Fig. 1 Schematic cross-section of the simulated device with an abrupt (a) and graded-layer (b) heterojunction. (c) Comparison of the simulated band structures. (d) Comparison of the simulated room temperature  $I$ - $V$  characteristics.

To test this hypothesis, three different Schottky barrier diode structures were grown: a control sample with a homoepitaxial AlN contact layer, a device with an abrupt heterojunction, and a device with a graded-layer heterojunction. The drift layers for all the diodes were 1  $\mu\text{m}$  thick and doped at  $[\text{Si}] = 1 \times 10^{18} \text{ cm}^{-3}$ . For the control device, the contact layer consisted of a 1  $\mu\text{m}$  thick  $n^+$ -AlN layer with  $[\text{Si}] = 1 \times 10^{19} \text{ cm}^{-3}$ , while the contact layers for the heterojunction devices consisted of a 2  $\mu\text{m}$  thick  $n^+$ -Al<sub>0.75</sub>Ga<sub>0.25</sub>N with  $[\text{Si}] = 1 \times 10^{19} \text{ cm}^{-3}$ . The graded-layer heterojunction device had a 100 nm thick compositionally-graded layer between the contact and drift layers, which was doped with  $[\text{Si}] = 1 \times 10^{19} \text{ cm}^{-3}$ . The schematic cross-sections of the final fabricated devices are shown in Fig. 2.

The device layers were grown on c-oriented, single crystal AlN wafers (procured from HexaTech) in a vertical, low-pressure, radiofrequency-heated, metalorganic chemical vapor deposition reactor. The substrate had an average dislocation density of  $10^3 \text{ cm}^{-2}$ . Trimethylaluminum, triethylgallium, silane and ammonia were used as the Al, Ga, Si and N precursors, respectively. More details on the substrate preparation and subsequent AlN epitaxy can be found elsewhere.<sup>18,31–33</sup> The drift layer was confirmed by Hall measurements to have a carrier concentration, mobility, and resistivity of  $2 \times 10^{15} \text{ cm}^{-3}$ , 160  $\text{cm}^2/\text{Vs}$  and 26  $\Omega \cdot \text{cm}$ , respectively. The  $n^+$ -Al<sub>0.75</sub>Ga<sub>0.25</sub>N layer had a carrier concentration, resistivity, and mobility of  $9.8 \times 10^{18} \text{ cm}^{-3}$ , 24  $\text{cm}^2/\text{Vs}$  and 27  $\text{m}\Omega \cdot \text{cm}$ , respectively. Hall effect measurements were performed using an 8400 series Lakeshore AC/DC Hall measurement system with contacts in the van der Pauw configuration.

The device fabrication followed a photolithography process. First, circular mesas with radii ranging from 25 to 300  $\mu\text{m}$  were defined using photolithography and reactive-ion etching to expose the underlying AlGaN contact layer. The etch chemistry was  $\text{BCl}_3/\text{Cl}_2$  and the etch rate was 30 nm/min. Then, large area ( $>1 \text{ cm}^2$ ) ohmic contacts were formed by the electron beam evaporation of a Cr/Ti/Al/Ti/Au (20/20/100/45/55 nm) metal stack on the exposed contact layer surface, and subsequently annealed at 950°C for 30 s in a  $\text{N}_2$  atmosphere. Finally, the Schottky contact (Ni) was deposited on the AlN drift layer surface. The Schottky-ohmic contact spacing was 10  $\mu\text{m}$ ; 5  $\mu\text{m}$  from Schottky to mesa edge and 5  $\mu\text{m}$  from mesa to Ohmic. No edge termination was implemented for field management. The fabrication process was identical for all devices.  $I$ - $V$  and impedance spectroscopy measurements were performed using a Keithley 4200 semiconductor characterization system.  $I$ - $V$  measurements were performed on devices with  $r = 25 \mu\text{m}$ , whereas impedance measurements were performed on  $r = 300 \mu\text{m}$  devices. Note that the Ohmic contact area was

much larger than the Schottky contact area, so the contribution of the ohmic contact resistance to the total device resistance was negligible. Current scaling with the Schottky contact area in the  $I$ - $V$  curves was observed on diodes up to  $r = 50 \mu\text{m}$  for all samples. For diodes with  $r > 50 \mu\text{m}$ , the current density decreased with increasing device area in all samples.

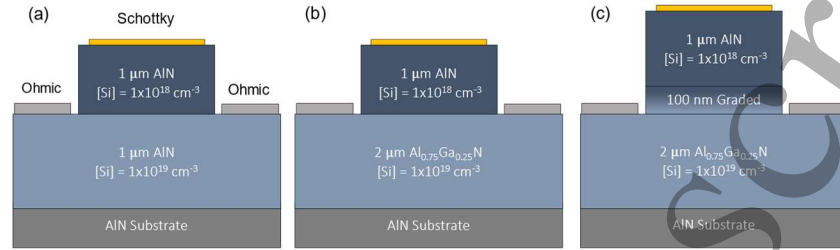


**Fig. 2** Schematic cross-sections of the fabricated AlN Schottky barrier diodes: (a) the control device, (b) the abrupt heterojunction device and (c) the graded-layer heterojunction device.

Figs. 3 (a) and (b) show the room temperature current-voltage ( $I$ - $V$ ) characteristics for the three fabricated Schottky barrier diodes on a semi-log and linear scale, respectively. From Fig. 3(a), all devices show a low ideality factor  $\leq 1.2$ , which indicates near-ideal Schottky diode behavior. Additionally, the devices show a large rectification ratio ( $I_{\text{ON}}/I_{\text{OFF}} > 10^{11}$ ). These results indicate that high quality Schottky contacts were realized, therefore, altering the composition of the underlying contact layer did not affect the formation of the Schottky contact. However, a clear effect of the ohmic contact layer on the output current is observed. The device with the graded-layer heterojunction showed significantly higher current than the other two diodes:  $10^3\times$  and  $10^4\times$  of that of the abrupt heterojunction and control devices, respectively. This can be more easily visualized by looking at the differential ON-resistance ( $R_{\text{ON}}$ ) vs. applied bias, which is shown for all devices in Fig. 3(c). The graded-layer heterojunction device shows the lowest  $R_{\text{ON}}$ ;  $< 1 \text{ m}\Omega \cdot \text{cm}^2$  after turn-on. This translates to current densities in the kA range, capable of being driven to current densities  $> 5 \text{ kA/cm}^2$  without failure. The other two devices show significantly higher  $R_{\text{ON}}$ , as shown in Fig. 3(a). These measurements are in good qualitative agreement with the simulated  $I$ - $V$  curves in Fig. 2(d). Therefore, the increased current capability in the graded-layer heterojunction device with respect to the abrupt device can be explained by the reduced parasitic electron barrier at the AlN/AlGa<sub>0.25</sub>N interface. The high  $R_{\text{ON}}$  in the control device can be understood in terms of the higher current spreading resistance of the underlying  $n^+$ -AlN contact layer, which has  $10^3\times$  higher resistivity than the  $n^+$ - $\text{Al}_{0.75}\text{Ga}_{0.25}\text{N}$  contact layer. These results highlight one of the main challenges in realizing AlN devices – in order to obtain high performance devices, the challenge of fabricating low resistance ohmic contacts to low-doped AlN must be solved.

It is interesting to note that for the graded heterojunction device, the differential  $R_{\text{ON}}$  is not constant after the device turns on. In fact, after 7 V forward bias, the observed  $R_{\text{ON}}$  reduces below the value expected from the resistivity of the AlN drift layer ( $2.6 \Omega \cdot \text{cm}^2$ ). This observed reduction in  $R_{\text{ON}}$  could be explained by a reduction in the resistivity of the AlN as a function of the applied voltage due to self-heating in the device. Since the Si donor has a high activation energy, as the device heats up, more Si will become ionized. For an activation energy of 0.3 eV, a  $50^\circ\text{C}$  increase in device temperature would result in roughly an order of magnitude increase in carrier concentration. This translates to

an order of magnitude decrease in the AlN resistivity, which is what is experimentally observed ( $0.6$  vs  $2.6 \Omega \cdot \text{cm}^2$ ). Since the device passes large current density, joule heating is a possible explanation for the observed lower specific on-resistance.

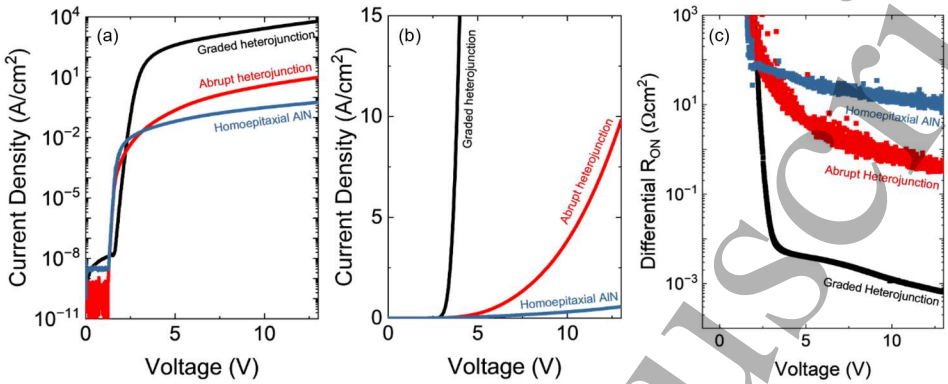


Fig. 3 Comparison of room temperature forward  $I$ - $V$  characteristics of the fabricated AlN Schottky barrier diodes with different ohmic contact layer structures on a semi-log scale. (b) Forward  $I$ - $V$  comparison on a linear scale. (c) Differential  $R_{ON}$  comparison for all devices shown on a semi-log scale.

According to the simulations shown in Fig. 2, the interface barrier should be reverse biased when the Schottky barrier is forward biased. Therefore, to provide further evidence for the parasitic electron barrier at the AlN/AlGaIn interface, impedance spectroscopy measurements were performed on the graded-layer and abrupt heterojunction devices. The measurements were made at frequencies ranging from 10 kHz to 10 MHz, with the applied bias ranging from -30 V to +30 V in 2.5 V steps. The corresponding Nyquist plots are shown in Figs. 4(a) and (b). In the reverse bias, the impedance spectra for both devices are consistent with a single parallel RC model and the capacitance follows a linear behavior in the  $1/C^2$ -V plot. To illustrate this, the capacitance was extracted from the reverse bias impedance measurements and the corresponding  $1/C^2$ -V plots are shown in Fig. 4 (c). The effective doping concentration can be extracted from slope of this plot and is found to be  $N_D - N_A = 6 \times 10^{17} \text{ cm}^{-3}$  for both devices. This value is consistent with the value extracted from the temperature dependent Hall measurements for the AlN drift layer.<sup>14</sup> An offset in capacitance is observed between the graded and abrupt heterojunction devices in Fig. 4(c). The total capacitance is lower in the abrupt device, which causes an anomalously high built-in potential to be extracted. This lower capacitance can be explained by the capacitive contribution of the abrupt AlN/AlGaIn interface, which would add in series to the Schottky barrier and therefore reduce the total measured capacitance. Nevertheless, the impedance in the reverse bias is dominated by the Schottky barrier, and the observed capacitance modulation corresponds to the modulation of the space-charge layer at the metal-semiconductor interface.

On the other hand, in the forward bias, the Schottky barrier is reduced and impedance contributions from other elements can be observed. For example, for the abrupt heterojunction diode, a second bias-dependent RC element appeared in the impedance spectra after the device turned on. This corresponded to the forward bias range of 5 to 30 V, as shown in Fig. 4(a). These results are consistent with the expected behavior of an electron barrier at the AlN/AlGaIn interface. Therefore, this second RC element can be interpreted as the impedance contribution of the reverse-biased AlN/AlGaIn junction. In contrast, the graded-layer heterojunction device did not show this behavior,

as seen in Fig. 4(b). Instead, series resistance contributions from both the AlN drift layer and the spreading resistance of the contact layer were observed. The absence of a second RC element indicated that the AlN/AlGaIn interfacial barrier was significantly reduced or completely removed by the introduction of the compositionally-graded interlayer. Therefore, these experimental results provide further evidence for the existence of a parasitic electron barrier at the AlN/AlGaIn interface and support the hypothesis that the increased current in the graded-layer heterojunction device stems from the reduction or removal of this barrier.

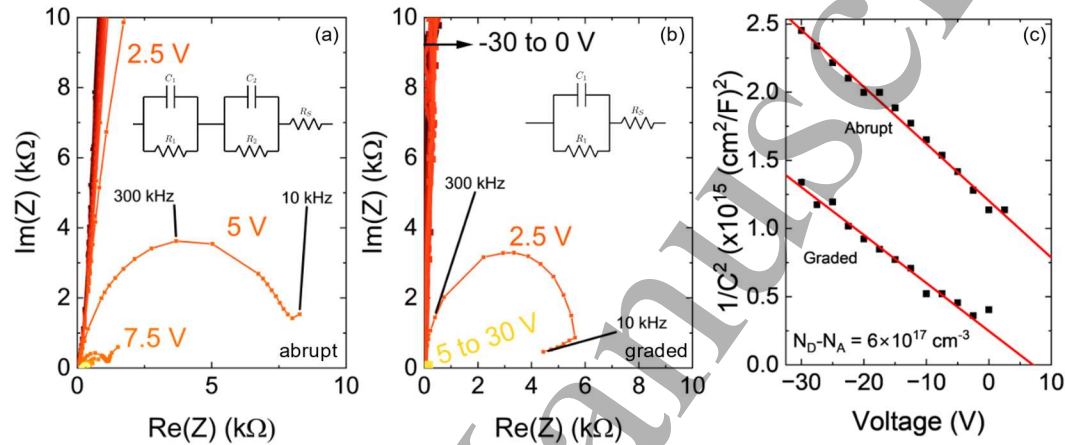


Fig. 4 Nyquist plots in forward bias for the device with an abrupt (a) and graded-layer heterojunction (b). The insets show the proposed equivalent circuits for each of the diodes. (c)  $1/C^2$ -V plot for both devices using the extracted capacitance from the impedance spectroscopy measurements in the reverse bias.

Based on the previous analysis, the influence of the parasitic elements was found to be negligible under the reverse bias. Therefore, the properties of the AlN drift layer can be investigated in this bias range. For the graded-layer heterojunction diode, it provides a unique opportunity to study the breakdown field of the AlN drift layer. The reverse bias  $I$ - $V$  characteristics for this device are shown in Fig. 5. The breakdown voltage was found to be  $V_{BD} = 680$  V, as shown in Fig. 5(a). Here,  $V_{BD}$  is defined as the voltage at which the current density reaches  $10^{-3}$  A/cm $^2$  in reverse bias. For comparison, the reverse bias  $I$ - $V$  characteristics for the same device were simulated using TCAD. The simulated breakdown voltage was found to be  $V_{BD} = 717$  V, in very good agreement with the experimental value of 680 V. To estimate the breakdown field in the AlN drift layer, the simulated electric field profile at 680 V reverse bias is shown in Fig. 5(b). From the graph, the maximum electric field at the experimental breakdown voltage was 12.3 MV/cm. It is worth emphasizing that no intentional field management was implemented in this device structure.



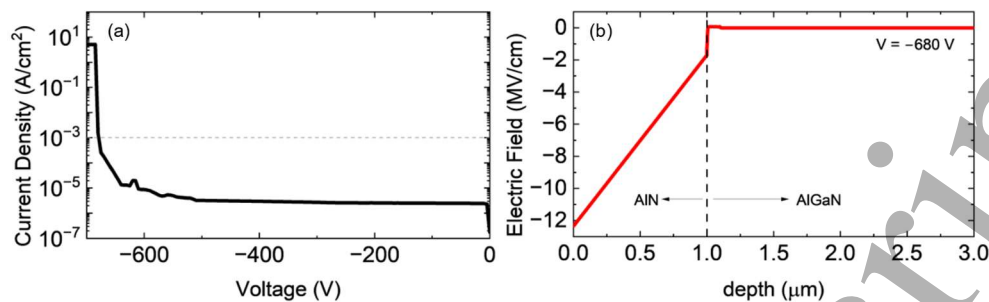


Fig. 5 (a) Reverse bias  $I$ - $V$  characteristics for the graded-layer heterojunction device showing a breakdown voltage of 680 V. (b) Simulated electric field profile for the same device, showing a maximum electric field of 12.3 MV/cm.

In conclusion, we have shown that the formation of low resistance ohmic contacts was crucial to device performance. Specifically, it was found that using an AlGaIn contact layer to AlN introduced an electron barrier arising from the band offsets between the two materials. This parasitic barrier was found to severely limit the forward current in fabricated devices, as it became reverse biased when the Schottky barrier was forward biased. By implementing a compositionally-graded interlayer between the contact and drift layers, a  $10^3\times$  increase in the forward current density was observed. With this device structure, AlN Schottky barrier diodes with state-of-the-art performance were demonstrated, as evidenced by a low ideality factor (1.2), low  $R_{ON}$  ( $<0.6\text{ m}\Omega\cdot\text{cm}^2$ ), high current density ( $>5\text{ kA/cm}^2$ ), and a large breakdown voltage (680 V).

The authors gratefully acknowledge funding in part from ARO (W911NF-22-2-0171), AFOSR (FA9550-17-1-0225, FA9550-19-1-0114), ARPA-E (DE-AR0001493), and NSF (ECCS-1916800, ECCS-1653383, ECCS-2145340). C.E. Quiñones was supported by the NASA Space Technology Graduate Research Opportunity (NSTGRO 80NSSC22K1198).

<sup>1</sup> B.J. Baliga, *Fundamentals of Power Semiconductor Devices* (Springer US, Boston, MA, 2008).

<sup>2</sup> J.Y. Tsao, S. Chowdhury, M.A. Hollis, D. Jena, N.M. Johnson, K.A. Jones, R.J. Kaplar, S. Rajan, C.G. Van de Walle, E. Bellotti, C.L. Chua, R. Collazo, M.E. Coltrin, J.A. Cooper, K.R. Evans, S. Graham, T.A. Grotjohn, E.R. Heller, M. Higashiwaki, M.S. Islam, P.W. Juodawlkis, M.A. Khan, A.D. Koehler, J.H. Leach, U.K. Mishra, R.J. Nemanich, R.C.N. Pilawa-Podgurski, J.B. Shealy, Z. Sitar, M.J. Tadjer, A.F. Witulski, M. Wraback, and J.A. Simmons, "Ultrawide-Bandgap Semiconductors: Research Opportunities and Challenges," *Adv. Electron. Mater.* **4**(1), 1600501 (2018).

<sup>3</sup> H. Amano, R. Collazo, C.D. Santi, S. Einfeldt, M. Funato, J. Glaab, S. Hagedorn, A. Hirano, H. Hirayama, R. Ishii, Y. Kashima, Y. Kawakami, R. Kirste, M. Kneissl, R. Martin, F. Mehnke, M. Meneghini, A. Ougazzaden, P.J. Parbrook, S. Rajan, P. Reddy, F. Römer, J. Ruschel, B. Sarkar, F. Scholz, L.J. Schowalter, P. Shields, Z. Sitar, L. Sulmoni, T. Wang, T. Wernicke, M. Weyers, B. Witzigmann, Y.-R. Wu, T. Wunderer, and Y. Zhang, "The 2020 UV emitter roadmap," *J. Phys. D: Appl. Phys.* **53**(50), 503001 (2020).

<sup>4</sup> A.G. Baca, A.M. Armstrong, B.A. Klein, A.A. Allerman, E.A. Douglas, and R.J. Kaplar, "Al-rich AlGaIn based transistors," *Journal of Vacuum Science & Technology A* **38**(2), 020803 (2020).

<sup>5</sup> J. Hyun Kim, P. Bagheri, R. Kirste, P. Reddy, R. Collazo, and Z. Sitar, "Tracking of Point Defects in the Full Compositional Range of AlGaIn via Photoluminescence Spectroscopy," *Physica Status Solidi (a)* **220**(8), 2200390 (2023).

<sup>6</sup> Z. Bryan, I. Bryan, B.E. Gaddy, P. Reddy, L. Hussey, M. Bobea, W. Guo, M. Hoffmann, R. Kirste, J. Tweedie, M. Gerhold, D.L. Irving, Z. Sitar, and R. Collazo, "Fermi level control of compensating point defects during metalorganic chemical vapor deposition growth of Si-doped AlGaIn," *Appl. Phys. Lett.* **105**(22), 222101 (2014).

<sup>7</sup> S. Washiyama, P. Reddy, B. Sarkar, M.H. Breckenridge, Q. Guo, P. Bagheri, A. Klump, R. Kirste, J. Tweedie, S. Mita, Z. Sitar, and R. Collazo, "The role of chemical potential in compensation control in Si:AlGaIn," *Journal of Applied Physics* **127**(10), 105702 (2020).

<sup>8</sup> J. Simon, A. (Kejia) Wang, H. Xing, S. Rajan, and D. Jena, "Carrier transport and confinement in polarization-induced three-dimensional electron slabs: Importance of alloy scattering in AlGaIn," *Appl. Phys. Lett.* **88**(4), 042109 (2006).

<sup>9</sup> J. Simon, V. Protasenko, C. Lian, H. Xing, and D. Jena, "Polarization-Induced Hole Doping in Wide-Band-Gap Uniaxial Semiconductor Heterostructures," *Science* **327**(5961), 60–64 (2010).



- <sup>10</sup> S. Rathkantiwar, P. Bagheri, D. Khachariya, J.H. Kim, Y. Kajikawa, P. Reddy, S. Mita, R. Kirste, B. Moody, R. Collazo, and Z. Sitar, "On the conduction mechanism in compositionally graded AlGaIn," *Appl. Phys. Lett.* **121**(7), 072106 (2022).
- <sup>11</sup> S. Rathkantiwar, P. Reddy, B. Moody, C. Quiñones-García, P. Bagheri, D. Khachariya, R. Dalmau, S. Mita, R. Kirste, R. Collazo, and Z. Sitar, "High p-conductivity in AlGaIn enabled by polarization field engineering," *Applied Physics Letters* **122**(15), 152105 (2023).
- <sup>12</sup> S. Agrawal, L. van Deurzen, J. Encomendero, J.E. Dill, H. Wei (Sheena) Huang, V. Protasenko, H. (Grace) Xing, and D. Jena, "Ultrawide bandgap semiconductor heterojunction p-n diodes with distributed polarization-doped p-type AlGaIn layers on bulk AlN substrates," *Applied Physics Letters* **124**(10), 102109 (2024).
- <sup>13</sup> T. Kumabe, A. Yoshikawa, S. Kawasaki, M. Kushimoto, Y. Honda, M. Arai, J. Suda, and H. Amano, "Demonstration of AlGaIn-on-AlN p-n Diodes With Dopant-Free Distributed Polarization Doping," *IEEE Trans. Electron Devices* **71**(5), 3396–3402 (2024).
- <sup>14</sup> P. Reddy, M.P. Hoffmann, F. Kaess, Z. Bryan, I. Bryan, M. Bobea, A. Klump, J. Tweedie, R. Kirste, S. Mita, M. Gerhold, R. Collazo, and Z. Sitar, "Point defect reduction in wide bandgap semiconductors by defect quasi Fermi level control," *J. Appl. Phys.* **120**(18), 185704 (2016).
- <sup>15</sup> P. Reddy, S. Washiyama, F. Kaess, R. Kirste, S. Mita, R. Collazo, and Z. Sitar, "Point defect reduction in MOCVD (Al)GaIn by chemical potential control and a comprehensive model of C incorporation in GaN," *Journal of Applied Physics* **122**(24), 245702 (2017).
- <sup>16</sup> Y. Taniyasu, M. Kasu, and T. Makimoto, "Increased electron mobility in n-type Si-doped AlN by reducing dislocation density," *Appl. Phys. Lett.* **89**(18), 182112 (2006).
- <sup>17</sup> M.H. Breckenridge, P. Bagheri, Q. Guo, B. Sarkar, D. Khachariya, S. Pavlidis, J. Tweedie, R. Kirste, S. Mita, P. Reddy, R. Collazo, and Z. Sitar, "High n-type conductivity and carrier concentration in Si-implanted homoepitaxial AlN," *Appl. Phys. Lett.* **118**(11), 112104 (2021).
- <sup>18</sup> P. Bagheri, C. Quiñones-García, D. Khachariya, S. Rathkantiwar, P. Reddy, R. Kirste, S. Mita, J. Tweedie, R. Collazo, and Z. Sitar, "High electron mobility in AlN:Si by point and extended defect management," *Journal of Applied Physics* **132**(18), 185703 (2022).
- <sup>19</sup> H. Ahmad, Z. Engel, C.M. Matthews, and W.A. Doolittle, "p-type AlN based heteroepitaxial diodes with Schottky, Pin, and junction barrier Schottky character achieving significant breakdown performance," *Journal of Applied Physics* **130**(19), 195702 (2021).
- <sup>20</sup> H. Ahmad, Z. Engel, C.M. Matthews, S. Lee, and W.A. Doolittle, "Realization of homojunction PN AlN diodes," *Journal of Applied Physics* **131**(17), 175701 (2022).
- <sup>21</sup> C.E. Quiñones, D. Khachariya, P. Bagheri, P. Reddy, S. Mita, R. Kirste, S. Rathkantiwar, J. Tweedie, S. Pavlidis, E. Kohn, R. Collazo, and Z. Sitar, "Demonstration of near-ideal Schottky contacts to Si-doped AlN," *Applied Physics Letters* **123**(17), 172103 (2023).
- <sup>22</sup> H. Fu, I. Baranowski, X. Huang, H. Chen, Z. Lu, J. Montes, X. Zhang, and Y. Zhao, "Demonstration of AlN Schottky Barrier Diodes With Blocking Voltage Over 1 kV," *IEEE Electron Device Letters* **38**(9), 1286–1289 (2017).
- <sup>23</sup> D.H. Mudiyanse, D. Wang, B. Da, Z. He, and H. Fu, "High-voltage AlN Schottky barrier diodes on bulk AlN substrates by MOCVD," *Appl. Phys. Express* **17**(1), 014005 (2024).
- <sup>24</sup> T. Maeda, R. Page, K. Nomoto, M. Toita, H.G. Xing, and D. Jena, "AlN quasi-vertical Schottky barrier diode on AlN bulk substrate using Al<sub>0.9</sub>Ga<sub>0.1</sub>N current spreading layer," *Appl. Phys. Express* **15**(6), 061007 (2022).
- <sup>25</sup> T. Kinoshita, T. Nagashima, T. Obata, S. Takashima, R. Yamamoto, R. Togashi, Y. Kumagai, R. Schlessler, R. Collazo, A. Koukutu, and Z. Sitar, "Fabrication of vertical Schottky barrier diodes on n-type freestanding AlN substrates grown by hydride vapor phase epitaxy," *Appl. Phys. Express* **8**(6), 061003 (2015).
- <sup>26</sup> Q. Zhou, H. Wu, H. Li, X. Tang, Z. Qin, D. Dong, Y. Lin, C. Lu, R. Qiu, R. Zheng, J. Wang, and B. Li, "Barrier Inhomogeneity of Schottky Diode on Nonpolar AlN Grown by Physical Vapor Transport," *IEEE Journal of the Electron Devices Society* **7**, 662–667 (2019).
- <sup>27</sup> H. Okumura, Y. Watanabe, and T. Shibata, "Temperature dependence of electrical characteristics of Si-implanted AlN layers on sapphire substrates," *Appl. Phys. Express* **16**(6), 064005 (2023).
- <sup>28</sup> B. Sarkar, B.B. Haidet, P. Reddy, R. Kirste, R. Collazo, and Z. Sitar, "Performance improvement of ohmic contacts on Al-rich n-AlGaIn grown on single crystal AlN substrate using reactive ion etching surface treatment," *Appl. Phys. Express* **10**(7), 071001 (2017).
- <sup>29</sup> R. France, T. Xu, P. Chen, R. Chandrasekaran, and T.D. Moustakas, "Vanadium-based Ohmic contacts to n-AlGaIn in the entire alloy composition," *Applied Physics Letters* **90**(6), 062115 (2007).
- <sup>30</sup> S. Rathkantiwar, J. Houston Dycus, S. Mita, R. Kirste, J. Tweedie, R. Collazo, and Z. Sitar, "Pseudomorphic growth of thick Al<sub>0.6</sub>Ga<sub>0.4</sub>N epilayers on AlN substrates," *Appl. Phys. Lett.* **120**(20), 202105 (2022).
- <sup>31</sup> I. Bryan, Z. Bryan, S. Mita, A. Rice, J. Tweedie, R. Collazo, and Z. Sitar, "Surface kinetics in AlN growth: A universal model for the control of surface morphology in III-nitrides," *Journal of Crystal Growth* **438**, 81–89 (2016).
- <sup>32</sup> A. Rice, R. Collazo, J. Tweedie, R. Dalmau, S. Mita, J. Xie, and Z. Sitar, "Surface preparation and homoepitaxial deposition of AlN on (0001)-oriented AlN substrates by metalorganic chemical vapor deposition," *Journal of Applied Physics* **108**(4), 043510 (2010).
- <sup>33</sup> R. Dalmau, B. Moody, R. Schlessler, S. Mita, J. Xie, M. Feneberg, B. Neuschl, K. Thonke, R. Collazo, A. Rice, J. Tweedie, and Z. Sitar, "Growth and Characterization of AlN and AlGaIn Epitaxial Films on AlN Single Crystal Substrates," *J. Electrochem. Soc.* **158**(5), H530 (2011).